Article

Reactivity of damaged pyrimidines: formation of a Schiff base intermediate at the glycosidic bond of saturated dihydrouridine

Yajun Jian, Gengjie Lin, Lidia Chomicz, and Lei Li

J. Am. Chem. Soc., **Just Accepted Manuscript** • DOI: 10.1021/ja512435j • Publication Date (Web): 11 Feb 2015

Reactivity of Damaged Pyrimidines: Formation of a Schiff Base Intermediate at the Glycosidic Bond of Saturated Dihydrouridine

Yajun Jian,[†,⊥] Gengjie Lin,[†,⊥] Lidia Chomicz,[‖] and Lei Li [†‡]*

[†]Department of Chemistry and Chemical Biology, Indiana University-Purdue University Indianapolis (IUPUI), 402 North Blackford Street, Indianapolis, Indiana, 46202

[‡]Department of Biochemistry and Molecular Biology and Department of Dermatology, Indiana University School of Medicine, 635 Barnhill Drive, Indianapolis, Indiana 46202

[‖]Department of Chemistry, University of Gdansk, 80-308 Gdansk, Poland

lilei@iupui.edu

ABSTRACT: DNA glycosylases catalyze the first step of the base excision repair (BER) pathway. The chemistry used by these enzymes for deglycosylation has been largely considered as the chemistry of the oxocarbenium ion, e.g. direct rupture of the C1′-N1 bond resulting in an oxocarbenium ion intermediate. Here we present mechanistic studies revealing the 2′-deoxyribose isomerization and subsequent deglycosylation processes in two pyrimidine lesions: 5,6-dihydro-2′-deoxyuridine (dHdU) and 5,6-dihydrothymidine (dHT), formed via ionizing radiation damage to 2′-deoxycytidine and thymidine respectively under anoxic conditions. Acid or heat treatment of these two lesions leads to the production of two pairs of C1′ epimers containing a pyranose and a furanose respectively, indicating that both lesions favor the rupture of the C1′-O4′ bond, resulting in a Schiff base intermediate at the *N*-glycosidic bond. Such a Schiff base intermediate was trapped and characterized by either Pd catalyzed hydrogenation or thiol-mediated addition reaction. In contrast, in undamaged 2′-deoxyuridine and thymidine, reactions at elevated temperatures lead to the release of nucleobases most likely via the traditional oxocarbenium ion pathway. DFT calculations further support the experimental findings, suggesting that the oxocarbenium ion intermediate is responsible for the deglycosylation process if the integrity of the pyrimidine ring is maintained; while the Schiff base intermediate is preferred if the C5=C6 bond is saturated. Currently, the oxocarbenium ion pathway is indicated to be solely responsible for the deglycosylation in BER enzymes, our results suggest an alternative Schiff base mechanism which may be responsible for the repair of saturated pyrimidine damages.

INTRODUCTION

As the genetic information carrier, DNA is under constant environmental stresses, such as oxidizing chemicals and UV irradiation. In cells under constant oxidative stress, the deoxyribonucleosides in the genome can be oxidized to various products. Among the four deoxyribonucleosides, 2′-deoxyguanosine has the lowest redox potential, followed by 2′-deoxyadenosine.[1] 2′-Deoxyguanosine oxidation leads to the formations of 8-oxo-7,8-dihydro-2′-deoxyguanosine (8-oxo-dG) and formamidopyrimidine deoxyguanosine (Fapy•dG) as the two common products.[2] Besides guanine, other nucleobases can also be oxidized.[1] As a matter of fact, although 8-oxo-dG is often used as a biomarker for oxidative stress, it is usually not the most abundant 2′-deoxyribonucleoside oxidation product. For instance, in neoplastic human monocytes exposed to gamma rays, thymidine oxidation products, the four *cis* and *trans* diastereomers of 5,6-dihydroxy-5,6-dihydrothymidine (e.g. thymidine glycol), 5-formyl-2′-deoxyuridine and 5-(hydroxymethyl)-2′-deoxyuridine, were all revealed by a HPLC-MS/MS analysis to be more abundant than 8-oxo-dG.[3]

The oxidized purine and pyrimidine residues are generally small; their presence usually does not result in significant helical distortions. The primary repair mechanism for most of these oxidative lesions is via the base excision repair (BER) pathway, although if a lesion is bulky enough to result in a severe strand distortion, it can also be repaired by the nucleotide excision repair (NER) pathway.[4-9] As demonstrated by a recent seminal work by McKibbin et al.,[10] further oxidation of 8-oxo-dG produces guanidinohydantoin (Gh) and spiroiminodihydantoin (Sp) lesions, which are prone for amine modifications. The amine-modified Sps, if bulky, can be efficiently repaired by the NER pathway; while all Sp-amine adducts can be repaired by the BER pathway irrespective of size.

A DNA lesion repair by the BER pathway is initiated by DNA glycosylases, which recognize and remove a specific damaged base by hydrolyzing the *N*-glycosidic bond to generate an abasic site (AP).[9] This deglycosylation chemistry has been largely considered as the chemistry of the oxocarbenium ion, e.g. rupture of the *N*-glycosidic bond resulting in an accumulation of positive charge on O4′ at the sugar

ring during the transition state (Route A, Figure 1).[4] A Schiff base mechanism (Route B, Figure 1) was proposed together with the oxocarbenium ion pathway by Zoltewicz et al. in 1970 to offer possible mechanistic explanation for the acid-catalyzed hydrolysis of some purine nucleosides.[11] Cadet and Teoule observed the isomerization and anomerization of pyrimidic deoxyribonucleosides in 2 M $HClO_4$ via formation of a possible Schiff base intermediate, supporting the mechanism B.[12] However, careful analyses of the acid catalyzed hydrolysis of 2′-deoxycytidine and 2′-deoxyuridine by Shapiro et al. found that the reaction kinetics is consistent with a mechanism involving the formation of mono- and dications of the nucleoside, followed by rupture of the *N*-glycosidic bond. This finding supports the route A and rules out the involvement of the Schiff base intermediate.[13] This oxocarbenium ion chemistry shares a common themes with *O*-glycoside (polysaccharide) hydrolyses and has been considered as the paradigm for the deglycosylation process for more than forty years.[4,8]

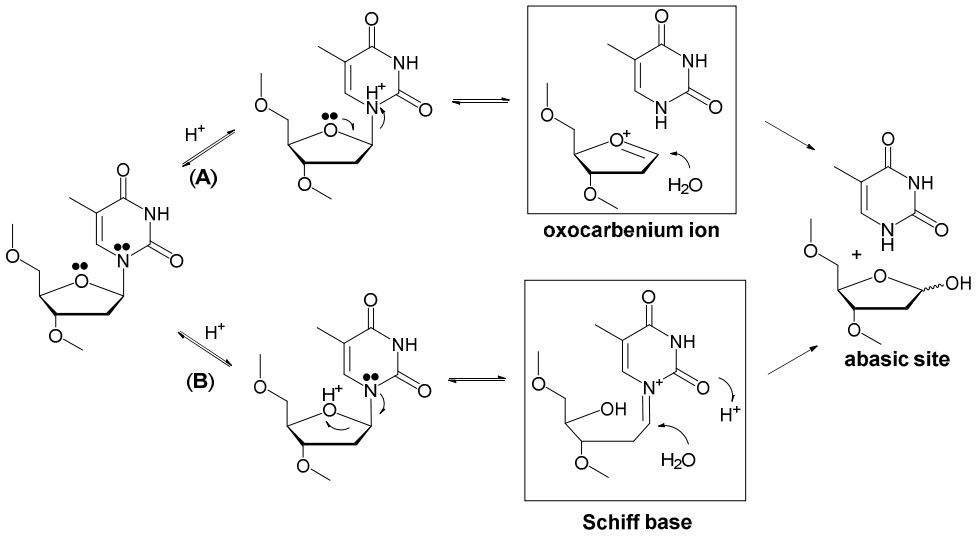

Figure 1. Two possible deglycosylation mechanisms proposed to date.

Analysis of Shapiro's data indicates that the conclusion was based on experiments using undamaged deoxyribonucleotides. It is known that nucleobase modifications may reduce their chemical stability, leading to novel reactions. Recently, our group has demonstrated that saturation of the thymine ring at the 5′-end of the 5-thyminyl-5,6-dihydrothymine, e.g. the spore photoproduct (SP), activates the C4=O moiety, supporting a water addition reaction to yield a hemiaminal intermediate.[14] In contrast, such a

reaction is not observed with an intact thymidine residue.[14] A similar reaction was observed with another damaged pyrimidine: 5,6-dihydro-2′-deoxyuridine (dHdU),[14] suggesting that this reaction may be ascribed as a general property of a saturated pyrimidine residue. Oxidation, alkylation, and other electrophilic reagents acting on nucleobases are known to reduce the electron density from the heterocycle, making the modified nucleobases better leaving groups to form an AP.[1] These observations indicate that the deglycosylation reaction occurs more readily after certain base modifications. We therefore wonder whether the reaction mechanism with modified nucleobases is truly the same as that revealed previously with intact deoxyribonucleosides.

We hereby used dHdU as the general model of a saturated pyrimidine residue to examine its chemical stability and reactivity, with hope to gain possible mechanistic insights into the deglycosylation process. It is worth mentioning that dHdU results from ionizing radiation damage to cytosine under anoxic conditions.[15,16] It is the third abundant pyrimidine damages in gamma irradiated genomic DNA, trailing only by 5-hydroxy-5-methylhydantoin and 5-hydroxy-5,6-dihydrouracil.[17] It is highly mutagenic at both replication and transcription levels.[18,19] Therefore, the dHdU research by itself is also of great significance. Our experimental results show that the Schiff base formation in route B becomes the mechanism in the isomerization reaction of dHdU; this route is feasible to result in a subsequent deglycosylation process. In contrast, in undamaged 2′-deoxyuridine, formation of the traditional oxocarbenium ion via route A is most likely responsible for the deglycosylation process. Similar reactions were observed with 5,6-hydrothymidine/thymidine residues. Further DFT calculation indicates that formation of oxocarbenium ion is favorable if the pyrimidine ring remains intact; while Schiff base is preferred once the C5=C6 bond is saturated. Therefore, both route A and route B are possible; their involvements in the cleavage of the *N*-glycosidic bond may be dependent on the nature of the deoxyribonucleotide lesions. The Schiff base mechanism has been discussed in bi-functional glycosylases which possess both glycosylase and AP lyase activities,[4,7,9] although it is not considered as a major contributor to the deglycosylation process.[4] Our report indicates that a saturated pyrimidine lesion thermodynamically prefers the Schiff base pathway. The bi-functional DNA glycosylases may

need to be re-examined to reveal whether the Schiff base pathway is indeed responsible for enzyme catalysis.

METHODS

Materials and General Methods. All solvents and chemicals were of analytical grade and purchased from Sigma-Aldrich, Fisher, or VWR and used without further purification. NMR spectra were obtained via a Bruker 500 MHz Fourier transform NMR spectrometer using deuterium oxide, d_4-methanol or d_6-DMSO as solvent with residual water/MeOH/DMSO acting as an internal standard. Mass spectrometric (MS) analyses were obtained via electrospray ionization (ESI) employing an ion-trap mass analyzer. High resolution MS and Tandem mass spectrometry (MS/MS) analyses were performed using a Q-TOF LC/MS spectrometer. The MS data were acquired via the "Agilent MassHunter Workstation Data Acquisition (B.03.00)" software and analyzed via "Qualitative Analysis of MassHunter Acquisition Data (B.03.00)" software.

Synthesis of dHdU. dHdU was synthesized via hydrogenation of the 2′-deoxyuridine as described in our previous work.[14]

dHdU isomerization reaction in 0.1 M HCl. dHdU was dissolved in 200 μL 0.1 M HCl to a final concentration of 85 mM. The resulting solution was maintained at room temperature for ~ 2 days. At various times, 5 μL of the reaction solution was aliquotted out, immediately frozen in liquid N_2, and saved in −20 °C freezer for future HPLC analysis. Four major products **1**, **2**, **3**, and **4** were generated from this reaction.

dHdU isomerization reaction at 90 °C in a pH 7.4 buffer. In a separate set of experiments, dHdU was dissolved in 200 μL pH 7.4 sodium phosphate buffer containing 150 mM NaCl to a final concentration of 85 mM. The solution was heated to 90 °C using a PCR device with a cap heating function to minimize water evaporation. At various reaction times, 5 μL solution was aliquotted out, immediately frozen in liquid N_2, and saved in −20 °C freezer for future HPLC analysis. Again, products **1**, **2**, **3**, and **4** were observed during a 3-day reaction.[20]

Determination of dHdU isomerization rate at 37 °C and pH 7.4. The dHdU solution in the pH

7.4 buffer as described above was heated to 90 °C, 85 °C, 80 °C, 75 °C and 70 °C respectively in the PCR device. At various reaction times, 5 μL solution was aliquotted out, immediately frozen in liquid N_2, and stored in –20 °C freezer for HPLC analysis. The formation rates of **1**, **2**, **3**, and **4** were determined by plotting the HPLC peak integrations against time at a given temperature. The extent of reaction was carefully controlled so that less than 10% of dHdU was consumed. Under such a situation, the dHdU concentration change is small and can be neglected in the rate constant calculation. Moreover, since formations of **2**, **3**, and **4** from dHdU are reversible, the small extent of reaction determines that the impact of these reverse processes can also be neglected. The rate constants were therefore calculated using the starting concentration of dHdU. Arrhenius plots for the dHdU reaction (lnk *vs* 1/T) were subsequently constructed and the formation rates for these products at 37 °C and pH 7.4 were deduced.[20]

Isomerization of 2′-deoxyuridine (dU) and thymidine (T) at pH 1. dU and T were dissolved respectively in 200 μL 0.1 M HCl to a final concentration of 85 mM. The resulting solution was kept at room temperature for ~ 3 days. At various times, 5 μL of the reaction solution was aliquotted out, immediately frozen in liquid N_2 and saved in –20 °C freezer for future HPLC analysis. No product was observed in either reaction.

Isomerization of dU and T at 90 °C in a pH 7.4 buffer. dU and T were dissolved respectively in 200 μL pH 7.4 sodium phosphate buffer with 150 mM NaCl to a final concentration of 85 mM. The solution was heated to 90 ºC using a PCR device with a cap heating function to minimize water evaporation. At various reaction times, 5 μL solution was aliquotted out, immediately frozen in liquid N_2, and saved in –20 °C freezer for future HPLC analysis. Uracil and thymine were observed in a 3-day reaction, indicating the rupture of the *N*-glycosidic bond. However, no isomers of dU or T were observed.[20]

Preparations of dHdU isomerization products in a large scale. HPLC analysis reveals that the acid or heat treatment of dHdU results in four products, including three dHdU isomers **2**, **3** and **4**. To

characterize these products, the reaction was repeated at a bigger scale. Briefly, 200 mg dHdU was dissolved in 0.1 M HCl and the reaction was allowed to proceed for 8 hours at ambient temperature. The products were separated via semi-preparative HPLC using procedures described below. The products were collected, concentrated, and desalted by reinjection into HPLC using H_2O-acetonitrile as elution buffers. The products were then characterized by MS/MS analysis and NMR spectroscopy.

Hydrogenation of the dHdU Schiff base intermediate. To further characterize the Schiff base intermediate possibly formed during the dHdU isomerization reaction, we attempted to trap this intermediate via a palladium-catalyzed hydrogenation reaction. Briefly, dHdU (50 mg, 0.22 mmol) was dissolved in 0.1 M HCl in MeOH:H_2O (1:1, v/v) solution to a final concentration of 5 mM (44 mL), 50 mg Pd-C was then added to the solution. The resulting suspension was stirred under 1 atm H_2 for 8 days at ambient temperature. At various time points, 5 µl of the reaction mixture was extracted, and immediately analyzed by HPLC until ~85% dHdU was consumed. After removing the Pd-C by filtration, the product was purified by semi-preparative HPLC to yield the hydrogenated dHdU (**5**) as a white solid (38 mg, 75%). Formation of the hydrogenated dHdU was confirmed by LC-MS/MS analysis and NMR spectroscopy.

Schiff base intermediate-mediated nucleophilic addition reaction. To shed light on the reactivity of the putative Schiff base intermediate formed in dHdU, we dissolved dHdU (20 mg, 85 µmol) in an aqueous solution at pH 3 to a final concentration of 60 mM. To this solution, 75 fold of cysteine also dissolved in pH 3 solution was added and the resulting solution allowed to react at 37 ºC. At various times, 5 µl of the reaction mixture was extracted, and immediately analyzed by HPLC. Two dHdU-cysteine adducts, **6** and **7**, were observed, as indicated by the LC-MS/MS. However, isolation of these products from the starting materials by semi-preparative HPLC is problematic, making it difficult for structural determination via NMR spectroscopy.

To facilitate product purification, we repeated the reaction using 75-fold 3-mercaptopropionic acid (MPA) as a cysteine analog. MPA retains the thiol moiety as the potential nucleophile, but lacks the α-

amino moiety in cysteine. Removal of the amino moiety drastically improves the HPLC chromatography; moreover, it eliminates the possibility for the amino moiety to serve as a potential competing nucleophile. The reaction solution was allowed to proceed at 37 ºC. At various times, 5 µl of the reaction mixture was extracted, and immediately analyzed by HPLC. At the end of the 8-day reaction, the products were purified by semi-preparative HPLC to afford the dHdU-MPA adducts **8** (10 mg, 30%) and **9** (18 mg, 56%) as colorless gel-like compounds.

HPLC Product Analyses. HPLC analyses were performed at room temperature using a Waters (Milford, MA) HPLC system coupled to a 2489 UV/visible detector at 230 nm. An Agilent ZORBAX Bonus-RP column (5 µm particle size, 250 × 4.6 mm i.d.) was equilibrated with buffer A (10 mM di-N-butylammonium acetate or 10 mM ammonium acetate aqueous solution, pH 7.0). Compounds were eluted with an ascending gradient of acetonitrile (buffer B) in 20 minutes at a flow rate of 1 mL/min.

The semi-preparative HPLC was performed at room temperature with the same Waters HPLC setup. An XBridge™ OST C18 column (2.5 µm particle size, 50 × 10 mm i.d.) was equilibrated with buffer A (10 mM ammonium acetate, pH 7.0), while compounds were eluted with an ascending gradient (0% ~ 5%) of acetonitrile (buffer B) in 20 minutes at a flow rate of 4.73 mL/min.

Product Analyses via Tandem Mass Spectrometry (MS/MS). MS/MS analyses of the reaction products were conducted using an Agilent 6520 Accurate Mass Q-TOF LC/MS spectrometer. The column was equilibrated in buffer A (5 mM ammonium acetate in 99% water and 1% acetonitrile, pH 6.5), while compounds were eluted with an ascending gradient (0% ~ 5%) of acetonitrile (buffer B) in 20 minutes at a flow rate of 0.5 mL/min. The mass signals were monitored under both positive and negative ion modes.

DFT calculations on the deglycosylation reactions of dU/dHdU and T/dHT. All calculations were conducted using the popular Becke's three-parameter hybrid functional B3LYP[21-23] and the 6-31++G(d,p) basis set,[24,25] with the Gaussian09 package.[26] Polarizable Continuum Model (PCM) was

used to mimic water environment.[27-29] The Gibbs free energy changes (ΔGs) describing considered reactions were the differences between the electronic energies of reactants and products, with entropy, zero-point vibrational, thermal and pV corrections. Thermodynamic terms were calculated at T = 298 K and p = 1 atm, in the rigid rotor-harmonic oscillator approximation.[30,31] ΔG for protonation of a nucleoside X into XH^+ was calculated as $\Delta G = (G_{XH+} + G_{H2O}) - (G_X + G_{H3O+})$, where each of given four reactants was optimized separately in PCM aqueous environment. Such a procedure allows us to calculate the thermodynamic effect of protonation, irrespective of the pH or reagents concentrations in solution.

We used C3′-endo conformation for deoxyribose ring and native anti conformation of nucleobase as the starting geometries of dU/dHdU and T/dHT. No geometrical constraints were used during geometry optimization and the analysis of harmonic frequencies demonstrated that all resulting structures were at their energetic minima (all force constants were positive).

RESULTS

Formation of Four Major Products under Acidic Conditions. Incubation of dHdU in 0.1 M HCl for 24 hrs at ambient temperature resulted in the formation of four products (**1**, **2**, **3**, and **4**, Figure 2A). ESI-MS analyses of these products (positive ion mode) revealed that **1** possesses an *m/z* value of 115.0, corresponding to the $[M + H]^+$ signal of the dihydrouracil. To confirm this observation, we co-injected commercially available 5,6-dihydrouracil with **1**. HPLC analysis confirms that these two compounds co-elute under the same peak. Therefore, one of the consequences for the dHdU acid treatment is the rupture of the *N*-glycosidic bond.

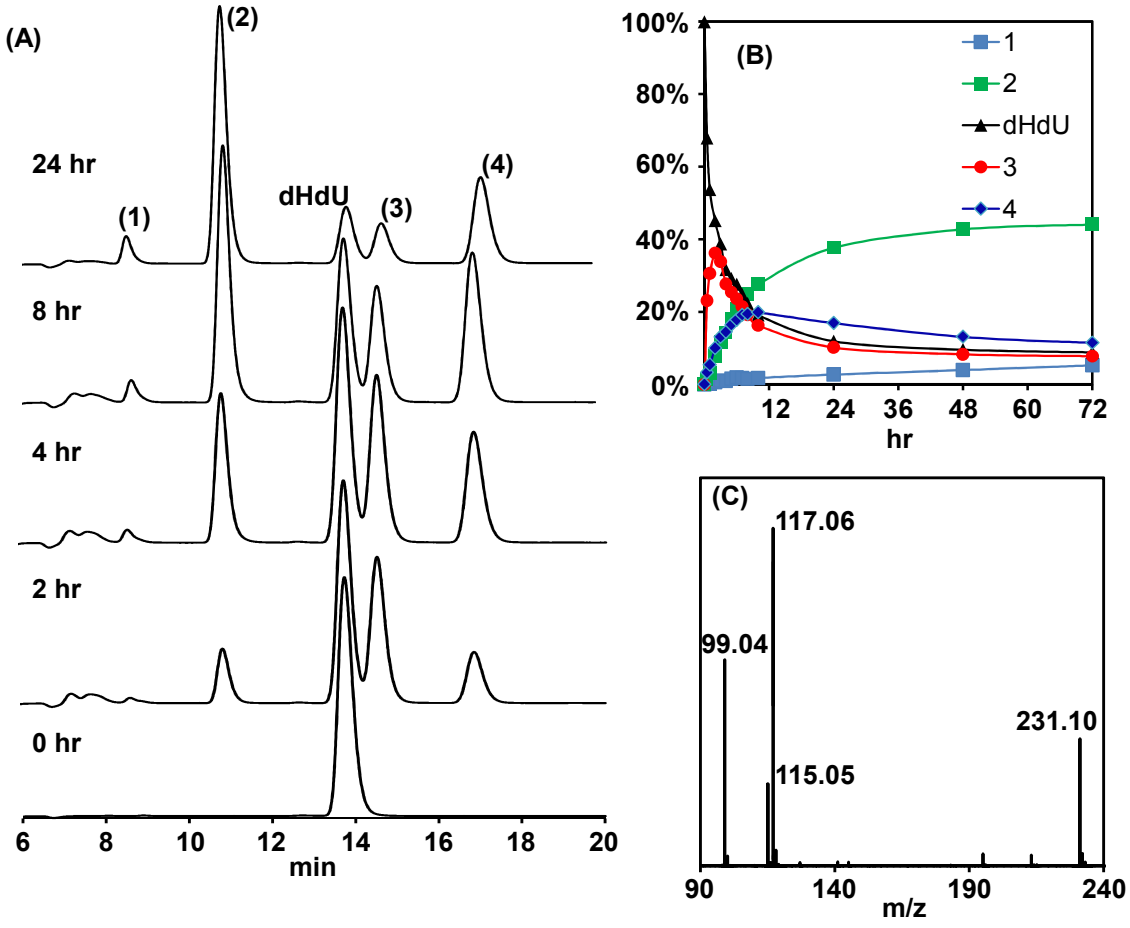

Figure 2. (A) HPLC chromatogram (monitored at 230 nm) of the dHdU isomerization reaction in the presence of 0.1 M HCl at ambient temperature for 24 hrs. (B) The formation kinetics for the dHdU isomerization reaction in 0.1 M HCl. It is obvious that formation of **3** is the kinetically most favorable reaction, and the formation of **2** is the thermodynamically most favorable reaction. (C) MS/MS analyses (positive ion mode, $[M + H]^+$) of dHdU. Identical fragmentation patterns were observed for products **2**,

3, and **4**; the mass spectra and the chemical structures of the fragments are shown in the SI.

ESI-MS analysis of products **2**, **3**, and **4** reveals that they all exhibit a *m/z* value of 231.1, which is the same as the $[M + H]^+$ signal of dHdU. The unchanged mass indicates that these three species are isomers of dHdU. As shown in Figure 2B, among the three products, **3** exhibits the fastest formation rate, suggesting that its formation is kinetically favorable. As the reaction proceeds, signals corresponding to **2** and **4** keep growing at the expense of dHdU and **3**. After 24 hrs, **2** and **4** become the major products. This observation suggests that formations of **2** and **4** are thermodynamically favorable. Moreover, the reaction appears to reach equilibrium in 72 hrs; prolonged incubation at ambient temperature in 0.1 M HCl does not lead to further change on the ratios among dHdU and its isomers.

Characterization of 2, 3 and 4 via MS/MS spectrometry. Formation of the deglycosylation product **1** together with dHdU isomers **2**, **3** and **4** indicates that the isomerization reaction may result from activation of the *N*-glycosidic bond. To shed light on the nature of this reaction, we first used MS/MS to analyze the product structures. As shown in Figure 2C, the fragmentation of dHdU results in three major peaks at m/z of 117.0, 115.0 and 99.0 Th respectively. The $[M + H]^+$ signal at 115.0 Th results from the release of 5,6-dihydouracil moiety; while the $[M + H]^+$ signal of 117.0 Th corresponds to the resulting 2′-deoxyribose moiety after loss of the dihydrouracil. Further elimination of the 3′-OH moiety at the deoxyribose by loss of a H_2O molecule may lead to the fragment of 99.0 Th. Structures of these fragments are shown in Figure S8 in the supporting information. The fragmentation patterns of **2**, **3** and **4** are indistinguishable from that of dHdU.[20] The fact that all these compounds exhibit a fragment with a $[M + H]^+$ signal at 115.0 Th suggests that the dihydrouracil ring is unchanged; the isomerization reaction likely occurs at the 2′-deoxyribose.

Characterization of 2, 3 and 4 via NMR spectroscopy. The MS/MS analysis supports the assumption that the dHdU isomerization reactions occur at the *N*-glycosidic bond. To further reveal the nature of these reactions, we determined the products' structures by 1D and 2D NMR spectroscopy. We

were able to assign all ^{1}H and ^{13}C NMR signals for dHdU and its isomers, which provide a solid foundation for structural determination. As shown in the HMBC spectra (Figure 3), H4′ interacts with C1′ in dHdU and **3**, suggesting that C1′ and C4′ are connected by the ether linkage as commonly found in a 2′-deoxyribofuranose. In contrast, in **2** and **4**, interactions between H5′/H5″ and C1′ were observed, indicating that C1′ and C5′ are linked. Therefore, **2** and **4** likely possess a 2′-deoxyribopyranose.

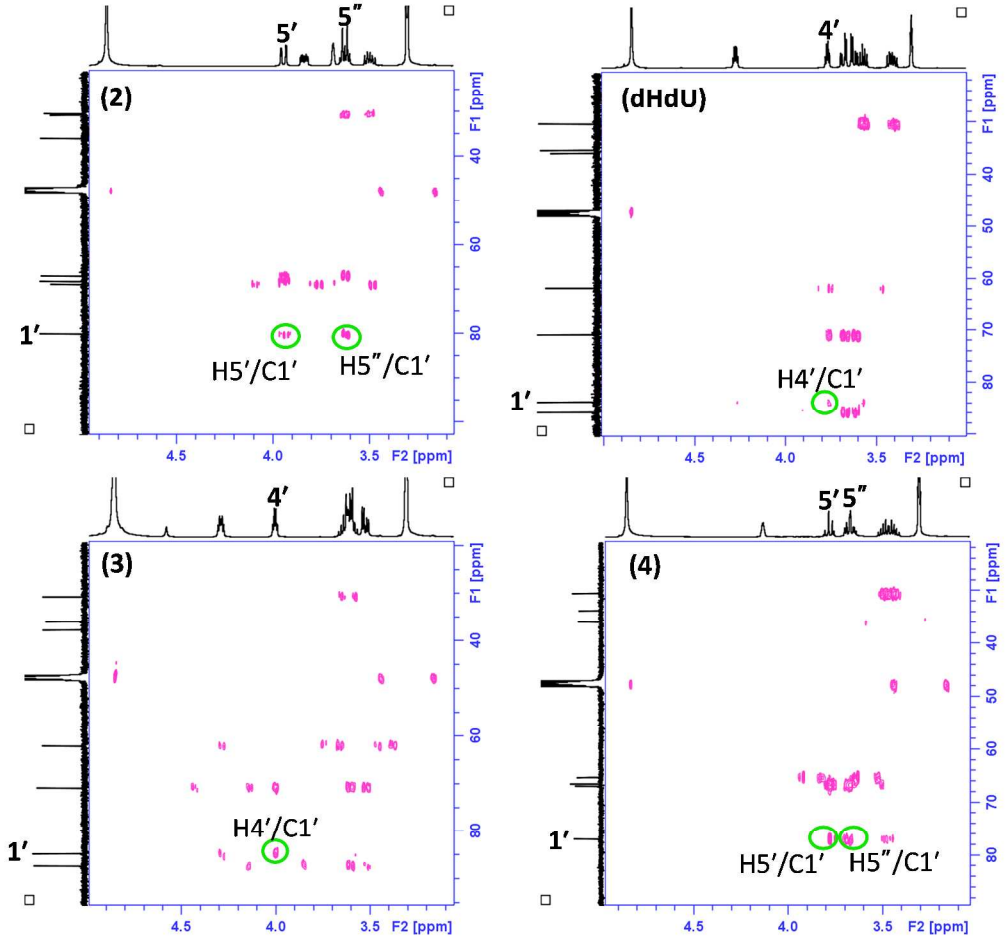

Figure 3. HMBC spectra for dHdU and its isomers **2**, **3** and **4**. Both dHdU and **3** exhibit an interaction between H4′ and C1′, indicating that they possess a deoxyribofuranose. In contrast, new HMBC signals were found in **2** and **4** for interactions between the two H5′ atoms and C1′, suggesting that C5′ and C1′ are connected by the ether bonds. Therefore, these two compounds likely possess a deoxyribopyranose.

These observations further indicate that the isomerization reaction occurs at the C1′ position. To reveal the nature of the reaction, we compared the NOE spectra of dHdU and **3** (Figure 4). In dHdU, both H2′ and H3′ were found to interact with H6 at the uracil ring, which is indicative of the naturally

occurring β-glycosidic bond. In contrast, both signals disappear in the NOE spectrum of **3**. Instead, **3** exhibits a signal owing to the H1′-H3′ interaction, suggesting that these two atoms are located on the same side of the furanose. Therefore, the *N*-glycosidic bond in **3** must adopt an α-configuration. In the NOE spectrum of **2**, interactions of H1′-H3′ and H2″-H6 were observed, indicating the presence of an α-glycosidic bond. While in **4**, H2′-H4′ and H2′-H6 were found to interact, which is consistent with the existence of a β-glycosidic bond. Taken together, the NMR data suggest that the acid treatment of dHdU produces two pairs of C1′ anomers possessing a pyranose and a furanose respectively (Scheme 1).

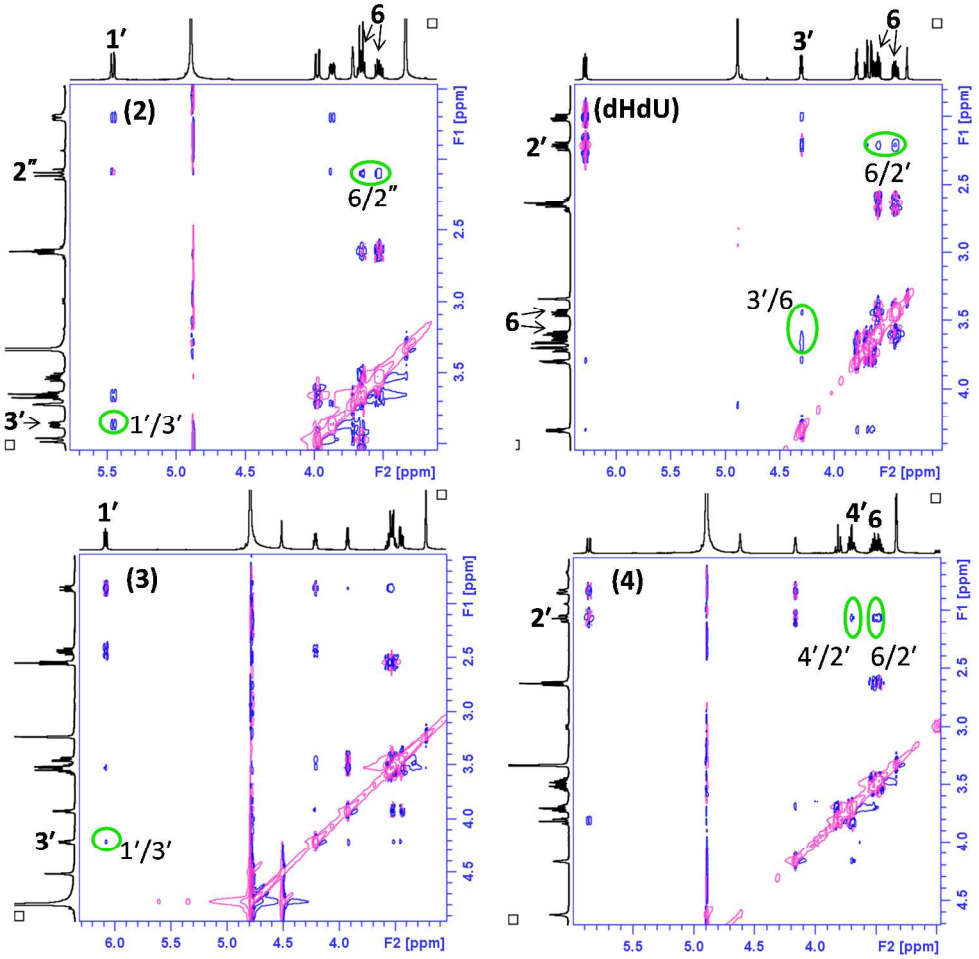

Figure 4. NOE spectra for dHdU and its isomers **2**, **3** and **4**. In dHdU and **4**, H2′ was found to interact with H6 at the uracil ring, indicating that both compounds contain a β-glycosidic bond. The additional interactions between H3′-H6 in dHdU and between H2′-H4′ in **4** further support this assignment. The H1′-H3′ interaction in **2** and **3** indicates an α-glycosidic bond in these complexes.

Scheme 1

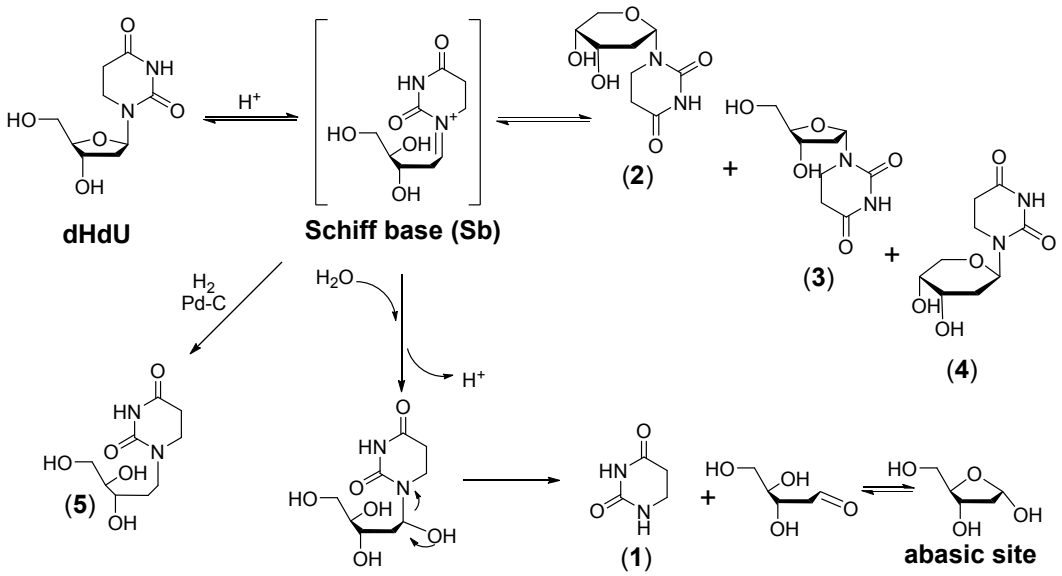

Formations of **2**, **3** and **4** can be best rationalized by the generation of a Schiff base intermediate (**Sb**) at the *N*-glycosidic bond (Scheme 1). Both the 4′-OH and the 5′-OH moieties can undergo nucleophilic addition to the C1′ position of **Sb** during the ring re-closure process. Moreover, such addition reactions can happen from either side of the $C=N^+$ bond, resulting in two pairs of C1′ epimers in dHdU/**3** and **2**/**4**. Formation of **3** containing an α-furanose requires relatively small conformational changes from dHdU. Moreover, 5-membered ring is considered as the most kinetically favorable configuration in ring closure reactions owing to the lowest entropic cost and transition state strain energy.[32,33] Therefore, it is not surprising that **3** exhibits the fastest formation kinetics among the three isomers (Figure 2B). On the other hand, 6-membered pyranose form generally dominates in aqueous solution over the five membered furanose form due to the enhanced thermal stability,[34] explaining the higher yields for **2** and **4** after a prolonged incubation. Between the two pyranose anomers, the α-anomer is generally more stable than the *β*-form due to the so-called anomeric effect,[35] explaining the higher yield of **2** than its epimer **4**.

The presence of a possible Schiff base intermediate **Sb** also offers an explanation for the generation

of the deglycosylation product **1**. In **Sb**, the C1′ position is electron deficient, and thus prone for the nucleophilic attack by a water molecule. The resulting water adduct is not stable; it readily undergoes an elimination reaction, releasing the dihydrouracil and generating an abasic site. Such a mechanism resembles the reaction route B in Figure 1, indicating that besides the traditional oxocarbenium ion pathway, the Schiff base mechanism may also be involved in the deglycosylation process under certain circumstances.

To trap the Schiff base intermediate via hydrogenation. To further characterize this Schiff base formation reaction, we attempted to trap the **Sb** intermediate. $NaBH_4$ is a common reagent used to trap Schiff base intermediates.[36-40] The reaction can be conducted in an aqueous buffer at the neutral pH. It is usually finished within an hour; decomposition of $NaBH_4$ is thus not a severe problem. In contrast, the dHdU isomerization requires a strong acidic condition and it takes several days for the isomerization reaction to reach completion. Under such a reaction condition, the $NaBH_4$ readily decomposes by reacting with H^+, releasing H_2. Thus, it is unsuitable to be used as a **Sb** trapping reagent.

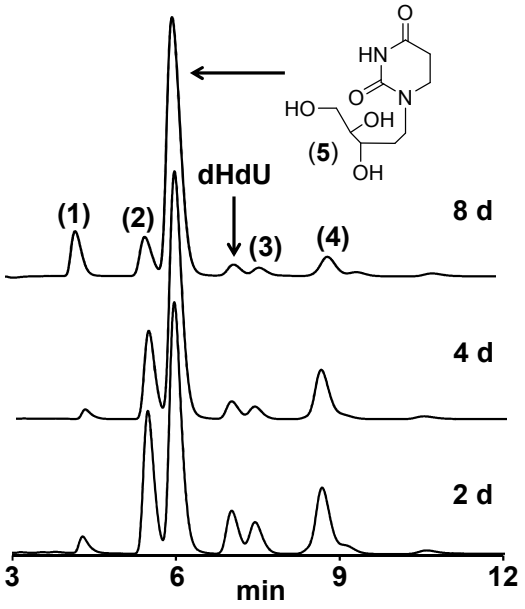

Figure 5. (A) HPLC chromatograms (monitored at 230 nm) of the dHdU hydrogenation in 0.1 M HCl for a reaction time of up to 8 days. The dHdU isomerization and deglycosylation reactions still occur under this acidic environment, as reflected by the formations of products **1**–**4**. The **Sb** hydrogenation product (**5**) is already the dominant species after a 2-day reaction. **5** continues to increase along with the deglycosylation product **1**; while the amounts of dHdU and its isomers **2**, **3** and **4** keep decreasing

during the 8-d reaction. This observation is consistent with the mechanism shown in Scheme 1: dHdU and its isomers are inter-convertible through the **Sb** intermediate; while the deglycosylation and **Sb** hydrogenation reactions yielding **1** and **5** respectively are irreversible processes.

After surveying a number of conditions, we found that 10% Pd/C can catalyze the hydrogenation of **Sb** at pH 1 and room temperature, yielding compound **5** in ~ 85% yield after a 8-day reaction (Scheme 1 and Figure 5). ESI-MS analysis reveals that **5** exhibits a $[M + H]^+$ signal at 233.1 Th, which is + 2 Th comparing with that from dHdU.[20] **5** was isolated by HPLC and characterized by NMR spectroscopy. In the ^{1}H NMR spectrum taken in MeOD, twelve carbon-based protons were found to be associated with **5**, contrasting to the eleven protons on dHdU. If the spectrum is taken in d_6-DMSO to enable the observation of exchangeable protons, three protons owing to 3′, 4′- and 5′-OH were found in **5**.[20] All these spectroscopic data support the chemical structure shown in Figure 5.

dHdU isomerization reaction at physiological pH. The results above support the **Sb** formation upon acid treatment. Such an acidic condition however does not exist in cells. As shown by Scheme 1, **Sb** formation is driven by the protonation of the O4′ moiety. The O4′ on 2′-deoxyribose is a weak base, whose protonation requires a strong acidic environment. *In vivo*, such a condition may be fulfilled by electrostatic and/or H-bonding interactions with amino acid residues on a glycosylase protein.[4,7-9] As a hydrogen bond may provide 1.8 ~ 3 kcal/mole stablization energy,[41,42] and the average energy contribution from a salt bridge is ~ 3.0 kcal/mole,[43] stabilization of the **Sb** intermediate can be readily achieved by these interactions within an enzyme. Moreover, in uracil DNA glycosylase, a theoretical computation indicates that the oxocarbenium ion intermediate is stabilized by the anionic phosphate groups from four nucleotides on the DNA substrate by 21.9 kcal mol^{-1};[44] experimental data suggest that the phosphodiester interactions with the substrate contribute 6-8 kcal/mole toward lowering the activation barrier.[45] It is reasonable to assume that the polyanionic DNA backbone may also provide significant stabilization of the **Sb** intermediate if it is indeed utilized by DNA glycosylases for catalysis.

Such stabilization networks do not exist in a non-protein environment. As the consequence, the **Sb**

population is likely to be very small at physiological pH. To shed light on whether the **Sb** formation can be achieved at the neutral pH, we accelerated the reaction by heating dHdU dissolved in pH 7.4 phosphate buffer to 90 °C. All three dHdU isomers as well as the cleaved dihydrouracil (**1**) were observed.[20] Although the reaction yields were lower than those observed at pH 1 and the reaction may not reach completion in 3 days, the data unambigiously prove that the **Sb** formation can ocurr at physicological pH. Via Arrhenius plots, the respective rate constants for the formations of **1**, **2**, **3** and **4** were calculated to be 0.82, 7.0, 54, and 1.9×10^{-9} s^{-1} at 37 °C. Again, the α-furanose product **3** is clearly the kinetically most favorable product.

Thiol addition to the C1′ position due to the Sb formation. As rationalized above, the Schiff base intermediate may be stabilized by the protein network. The C1′ position of **Sb** is electron difficient, which may support nucleophilic addition reactions by amino acids such as lysine and cysteine. However, if not located on a protein, the ε-NH_2 moiety in lysine is protonated at pH 7 and the resulting cationic form is a very poor nucleophile. Moreover, even if the lysine ε-NH_2 group does add to the C1′ position, without the protection from the protein network, the resulting Schiff base is not stable. It is readily hydrolyzed to produce an abasic site and restore the lysine amino moiety. Such a reaction is indistinguishable from an oxocarbenium ion mediated deglycosylation reaction and is thus of little mechanistic significance. In contrast, a thiol group is more difficult to be protonated; the –SH can function as a reasonably good nucleophile in a slightly acidic environment. More importantly, should the Schiff base intermediate be invovled, the –SH moiety would be readily added to the C1′ position. The resulting tetrahedral species is expected to be stable enough to survive the acidic environment needed for the reaction, enabling a thorough product characterization to shed light on the reaction mechanism.

We therefore incubated 75-fold cysteine with 60 mM dHdU at pH 3. The acidic condition was chosen to faciliate the **Sb** formation. At the same time, the acidity is not too strong to protonate the –SH moiety, thus enabling the possible trapping of the Schiff base intermediate. Analysis by HPLC reveals

the gradual increase of two products **6** and **7** in a 3-day reaction. ESI-MS analysis under the negative ion mode reveals that both products possess a molecular mass of 350.1 Th, indicating that they are dHdU-cysteine adducts. MS/MS analysis reveals three major fragments with m/z of 105.0, 149.0 and 229.1 Th respectively for both products.[20] The 149.0 Th signal can be best explained as the ring-opened ribose fragment with an sulfide attached to the C1′ position.[20] The fragmentation patterns are identical for **6** and **7**, suggesting that they are likely epimers.

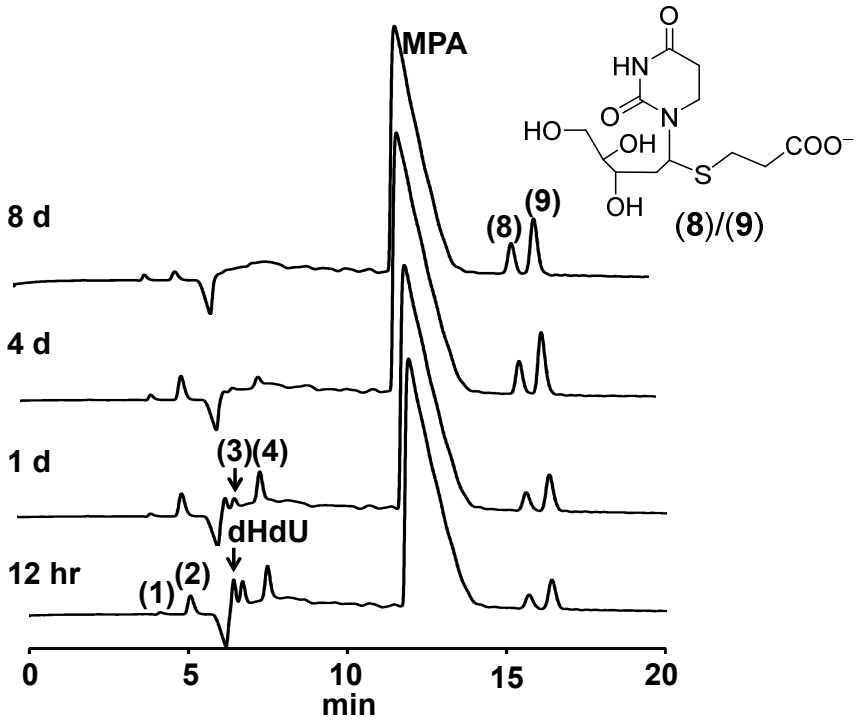

Figure 6. HPLC chromatograms (monitored at 230 nm) describing the formation of the dHdU-MPA adducts for a reaction of up to 8 days. The dHdU isomerization and deglycosylation reactions still occur under this acidic environment, as reflected by the formations of products **1**–**4**. The dHdU-MPA adducts (**8** and **9**) are already the major species after 12 hours; their yields continue to increase during the 8-d reaction at the expense of dHdU and its isomers. Please note that **8** and **9** differ at the chiral C1′ position; however we were unable to assign their absolute chiral configuration.

In the HPLC chromatogram, product **6** elutes immediately after the cysteine species, making it difficult to be purified by HPLC.[20] Moreover, although it is unlikely for the α-NH_2 group of cysteine to react given its high tendency to protonate resulting in the ammonium form under the strong acidic

condition, we would like to firmly exclude its involvement in the reaction. We therefore repeated the reaction using excess 3-mercaptopropionic acid (MPA). Ionization of MPA in water alters the pH to ~ 3, facilitating the Schiff base formation. As shown in Figure 6, this acidic condition induces formations of **Sb** and dHdU isomers. As the reaction proceeded, dHdU and its isomers became less and less, which was accompanied by the formation of two new products **8** and **9**.

In the ^{1}H NMR spectrum of **8** and **9**, all ^{1}H signals from dHdU and MPA remain, which is consistent with the hypothesis that they are dHdU-MPA adducts. We are unable to determine the absolute stereo-configuration for these two epimers via NOE spectroscopy due to the free rotation of the C1′-C2′ bond. This observation also agrees with the fact that the deoxyribofuranose ring at dHdU is opened. On the HMBC spectrum, the hydrogens at the γ-carbon of the MPA moiety exhibits a strong coupling with C1′, indicating that the sulfur from MPA is directly attached to the C1′ position.[20] Additionally, MS/MS analysis of **8** and **9** again exhibits three fragments with m/z of 105.0, 149.0 and 229.1 Th, which are same with those observed in the MS/MS analysis of dHdU-cysteine adducts **6** and **7**. Such an identical fragmentation pattern suggests that all thiol-adducts possess very similar structures. Taken together, all the spectroscopic data support our hypothesis that formation of **Sb** makes the C1′ position prone for nucleophilic addition reactions.

dHT isomerization reaction To ensure that the Schiff base formation is not a unique property of dHdU, we prepared 5*S*-dihydrothymidine (dHT) via hydrogenation of thymidine using a literature protocol.[43] We did not use 2′-deoxycytidine as the saturated C residue readily deaminates to dHdU.[46-48] This deamination reaction is drastically accelerated under an acidic or heated condition, making the saturated 2′-deoxycytidine unsuitable for the **Sb** formation studies. Upon treatment with 0.1 M HCl, three 5*S*-dHT isomers and the corresponding 5*S*-dihydrothymine residue were indeed generated, as indicated by the LC-MS/MS analysis.[20] The reaction closely resembles that obtained with dHdU, suggesting that the **Sb** formation is likely a general property of a saturated pyrimidine residue.

No isomerization was observed with dU or T To further confirm that the **Sb** formation is due to the saturated C5=C6 bond, we treated thymidine and 2′-deoxyuridine with 0.1 M HCl for 3 days. HPLC analysis confirms that no reaction occurs under such a condition.[20] Heating the thymidine or the 2′-deoxyuridine solution in a pH 7.4 phosphate buffer to 90 ºC for 3 days leads to the formation of thymine and uracil respectively; however, no corresponding thymidine or 2′-deoxyuridine isomers were observed.[20] These observations agree with the previous deglycosylation studies by Shapiro et al. using 2′-deoxyuridine and 2′-deoxycytidine,[13] indicating that thymidine and 2′-deoxyuridine deglycosylate via the traditional oxocarbenium ion pathway as shown in Figure 1A.

DFT calculations to understand the Sb formation Our observations thus suggest that both the Schiff base and the oxocarbenium ion intermediates shown in Figure 1 can be involved in the deglycosylation reactions. The oxocarbenium ion intermediate formation may be the dominant pathway if the aromaticity of the nucleobase is maintained; while the Schiff base route may be involved if the pyrimidine C5=C6 bond is saturated. To shed light on the possible reaction mechanism with different pyrimidine damages, we performed DFT calculations to compare the Gibbs free energy changes of these two reaction pathways.

Scheme 2

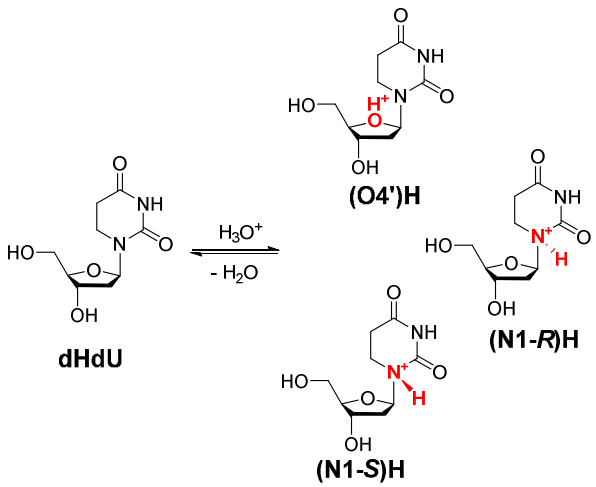

The deglycosylation process was suggested to be an acid-catalyzed reaction under physiologically

relevant conditions.[49,50] Indeed, our calculation found that the crucial step for this process is the protonation of the reacting nucleosides. If a proton is attached to a "right" position, the system energy is lower and bond cleavage may subsequently occur, leading to a corresponding product. We considered protonation at atoms with the lowest calculated Mulliken charges, namely at O4′ of the deoxyribose, as well as at N1, O2, N3, and O4 of the pyrimidine ring. Protonation at the last three positions (O2, N3, and O4) is omitted in the discussion as these atoms are mainly involved in hydrogen bonding interactions in duplex DNA and do not directly contribute to the deglycosylation process. Protonation at O4′ and N1 results in putative **(O4′)H**, **(N1-*R*)H**, and **(N1-*S*)H** intermediates respectively, as illustrated using dHdU in Scheme 2. We then compared the stability of these intermediates to reveal their tendency to further decay into Schiff base or oxocarbenium ion.

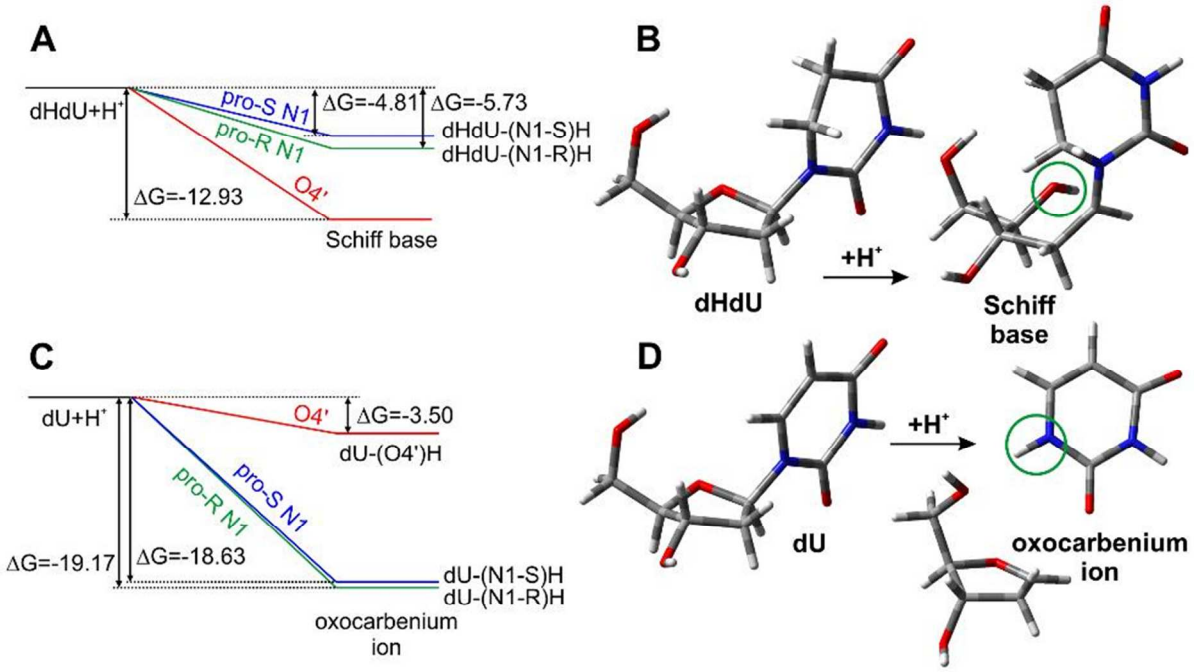

Figure 7. (A) Gibbs free energy changes (kcal/mol) for dHdU protonation and decomposition. Comparing with the general protonated dHdU state, the **(O4′)H** pathway which leads to the formation of Schiff base species lowers the free enthalpy by 7~ 8 kcal/mol more than the two putative N1 protonation pathways **(N1-*R*)H** and **(N1-*S*)H**. Therefore, in dHdU which contains a saturated C5=C6 bond, the Schiff base pathway is preferred over the traditional oxocarbenium ion pathway. (B) Geometry visualization of the optimized dHdU structure. After O4′ protonation, the resulting dHdU-**(O4′)H** is unstable, which transforms into the Schiff base via a barrier-free C1′-O4′ bond rupture during structure optimization. (C) Gibbs free energy changes (kcal/mol) for dU protonation and decomposition. Protonation at N1 produces either **(N1-*R*)H** or **(N1-*S*)H,** which decomposes into an oxocarbenium ion

via a barrier-free C1′-N1 breakage. Both N1-H species are lower in Gibbs free energy than the putative **(O4′)H**, suggesting that in dU where the ring aromaticity is maintained, the oxocarbenium ion pathway is heavily favored. (D) Geometry visualization of the optimized dU structure. dU protonated at N1 readily transforms into the oxocarbenium ion via a barrier-free C1′-N1 bond rupture. The newly attached protons in the resulting Schiff base (B) and oxocarbenium ion (D) are indicated by green circles.

As expected, the DFT calculations show that for a saturated pyrimidine nucleoside dHdU, protonation at the O4′ position of 2′-deoxyribose is preferred. The dHdU molecule with O4′ being protonated is unstable; it re-arranges into the Schiff base (**Sb**) during structural optimization via a barrier-free C1′-O4′ bond rupture. As we cannot accurately obtain the optimized **(O4′)H** structure during our calculation, we made a reasonable hypothesis, using that of **Sb** to estimate the Gibbs free energy change for the formation of **(O4′)H**. Such an approach allows us to obtain a Gibbs free energy change of -12.93 kcal/mol from the protonated dHdU state for the **(O4′)H** formation (Figure 7A). In contrast, protonation at the N1-*R* and N1-*S* position only lower the Gibbs free energy by -5.73 and -4.81 kcal/mol respectively. Therefore, the O4′ protonation is clearly the favorable pathway, indicating that in dHdU, the Schiff base formation is the preferred route (Figure 7B).

In contrast, in an undamaged nucleoside such as dU, protonation at the *pro-R* or *pro-S* position of N1 is clearly favored. Again, the **(N1-*R*)H** and **(N1-*S*)H** intermediates were found to be unstable; the C1′-N1 bond ruptures during structure optimization, leading to the formation of corresponding oxocarbenium ion species. The resulting oxocarbenium ions still maintain some conformational feature of their parent N1-H species, therefore possessing slightly different Gibbs free energy. Again, we used these oxocarbenium ions to estimate the free-enthalpy change of their parent N1-H species and found that the formations of **(N1-*R*)H** and **(N1-*S*)H** lead to Gibbs free energy changes of -19.17 and -18.63 kcal/mol respectively from the protonated dU state (Figure 7C). In contrast, the O4′ protonation is clearly unfavorable in dU, which only lowers the Gibbs free energy by -3.50 kcal/mol. Thus, in dU, the N1 protonation is the preferred pathway for deglycosylation, leading to the oxocarbenium ion formation (Figure 7D)

Similar trends are observed with the dHT and T deglycosylation processes respectively.[20] The Schiff base pathway is favored by 8.4 ~ 9.5 kcal/mol for dHT (Figure S13). For T, protonation at the N1-*R* position is favored; the resulting **(N1-*R*)H** subsequently transforms to the oxocarbenium ion via a barrier-free C1′-N1 bond rupture. In contrast, protonation at the N1-*S* position is a uphill process probably due to the steric hindrance; the formed putative **(N1-*S*)H** intermediate however is found to be metastable as a local minimum on the potential energy surface, which can be transformed into the oxocarbenium ion due to a favorable negative thermodynamic stimulus (~ – 27 kcal/mol, Gibbs free energy).[20] Despite this overall favorable thermodynamics, given the high energy barrier in the **(N1-*S*)H** pathway, we believe that the barrier-free **(N1-*R*)H** pathway is responsible for the oxocarbenium ion formation in T. Although such a stereo-selection may not be meaningful in our studies here, it could have biological indication if that happens in the binding pocket of a glycosylase as only one side of the pyrimidine ring may be favorable for the proton addition step to trigger the oxocarbenium ion formation.

DISCUSSION

Understanding details of the chemical reactivities of damaged DNA nucleobases is important in efforts aimed at lesion characterization, the chemical syntheses, the elucidation of possible biological repair routes, or the consequences of their persistence in a genome. The examples discussed here, dHdU and dHT, represent lesions resulting from ionizing radiation damage to C[11,12] and T[51] respectively. In cells, such lesions are removed by DNA glycosylases to initiate the damage repair process by the BER pathway.[4,7,9] The current paradigm governing this removal step is that the damaged base is detached by rupture of the N1-C1′ bond, leaving an oxocarbenium ion intermediate at the deoxyribose (Route A, Figure 1). Such an intermediate is commonly observed in the hydrolysis of glycans.[52-55] Moreover, using undamaged 2′-deoxyuridine and 2′-deoxycytidine, clear evidence was obtained that the *N*-glycosidic bond hydrolysis is mediated by the oxocarbenium ion pathway.[13] Although there were data supporting the involvement of a Schiff base intermediate resulting from the rupture of C1′-O4′ bond (Route B, Figure 1),[11,12] such a route is not considered to contribute to the deglycosylation process.[4]

Our report here, however, shows that in a saturated pyrimidine lesion such as dHdU and dHT, formation of the oxocarbenium ion cannot be observed; the reaction instead proceeds via the Schiff base pathway. In contrast, the oxocarbenium ion pathway is involved if the aromaticity at the pyrimidine ring is maintained, which is consistent with the previous 2′-deoxyuridine and 2′-deoxycytidine hydrolysis studies.[13] Our finding highlights the importance to maintain the integrity of the nucleobase ring. As shown in our previous work, loss of aromaticity in dHdU facilitates the formation of a hemiaminal intermediate at the C4 position;[14] such an intermediate cannot be observed in the undamaged thymine residue. Now we show that the C5=C6 saturation also surprisingly alters the stability of the remote 2′-deoxyribose, making the O4′ more readily to be protonated and promoting the Schiff base intermediate formation at the *N*-glycosidic bond. This result emphasizes the complicated impacts of a nucleobase modification to the overall reactivity of the nucleoside. Although the oxocarbenium ion intermediate is well established in the glycan chemistry and its formation was observed during the hydrolysis of intact

deoxyribonucleosides, the conclusion may still be misleading when applied to the studies of damaged nucleosides.

It is worth mentioning that acid-catalyzed ribose ring expansion/anomerization reactions were observed previously in saturated pyrimidine ribonucleosides or ribonucleoside analogs.[56-60] For instance, at pH 1, the β-furanose in tetrahydrouridine (THU) was found to quickly expand to a β-pyranose via a similar Schiff base intermediate; the ring expansion reaction, however, was not observed with uridine and dihydrouridine (dHU).[56] These observations partially agree with our dHdU reaction reported here, although it is puzzling that THU reaction only afforded the β-pyranose isomer, in contrast to the three isomers found in our dHdU reaction. Also, it is surprising that dHU did not isomerize. Spontaneous α-β anomerization was observed with the β-furanose attached to the reduced pyridine ring in nicotinamide adenine dinucleotide (NADH), but not with that in NAD^+ where the pyridine ring maintains its aromaticity.[57,58] These previous observations are largely consistent with our dHdU and dHT reactions, supporting our conclusion that once the pyrimidine ring aromaticity is lost, the attached (2′-deoxy)ribose is prone for the C1′ epimerization reaction via the Schiff base mechanism.

The Schiff base intermediate may also be observed with some purine damages. C1′ epimerization was observed in the synthesis of the phosphoramidites of Fapy•dG (*N*-(2′-deoxy-α,*β*-D-erythropentofuranosyl)-*N*-(2,6-diamino-4-hydroxy-5-formamidopyrimidine)) and Fapy•dA (N4-(2′-deoxy-α,β-D-erythropentofuranosyl)-4,6-diamino-5-formamidopyrimidine),[61-65] and posed a significant challenge for their incorporation into an oligonucleotide via solid phase synthesis. Although a Schiff base intermediate was proposed to explain the C1′ epimerization and facile isomerization reactions, previous discussions were mainly focused on the interference to the synthetic efforts for Fapy•dG or Fapy•dA incorporation. Given our data reported here, it is very likely that a similar Schiff base intermediate may exist in a naturally occurring Fapy•dG or Fapy•dA lesion formed in the genomic DNA. After facile protonation of the N7-position, a purine residue can be an excellent leaving group favoring the oxocarbenium ion formation.[4,66] It is unknown whether the Schiff base pathway is involved

in the depurination process in purine damages other than Fapy•dG and Fapy•dA.

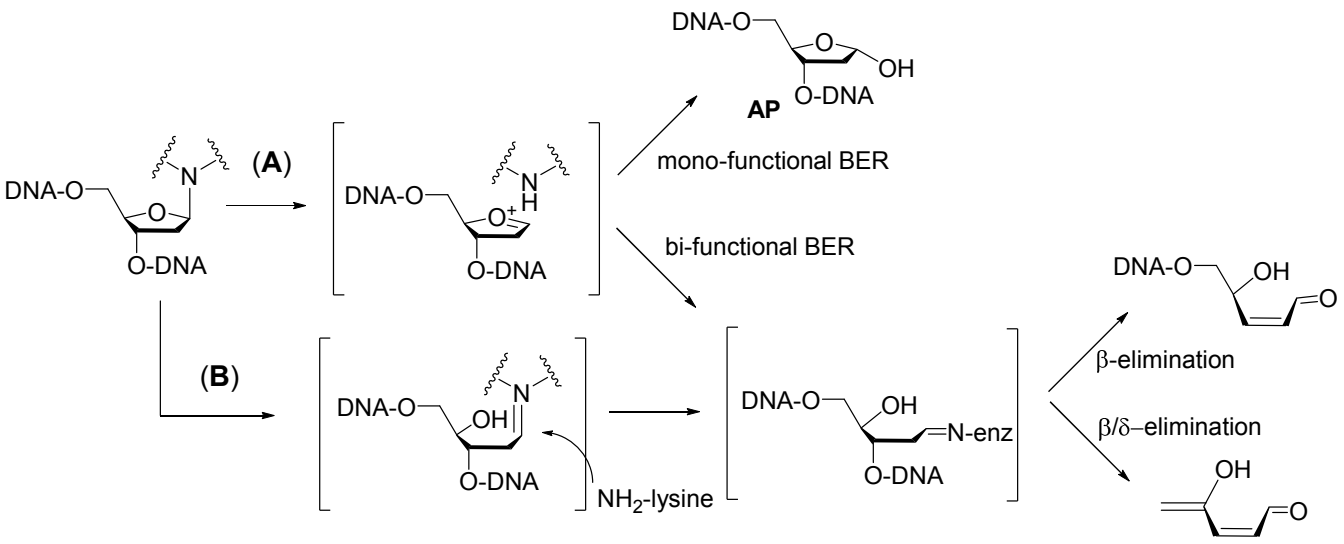

Figure 8. (A) Current mechanism for BER enzymes, which suggests that both mono-functional and bi-functional BER enzymes utilize the same oxocarbenium ion intermediate. In mono-functional BER enzymes, such an oxocarbenium ion formation leads to the direct removal of the damaged nucleobase. In bi-functional enzymes, the oxocarbenium ion intermediate subsequently reacts with an active-site lysine residue, resulting in a nucleoprotein complex connected by a Schiff base intermediate, which subsequently induces the β-elimination reaction and in some cases the β/δ-elimination reactions to cleave the DNA strand. (B) An alternative pathway for the bi-functional BER enzymes based on our Schiff base intermediate formation in this report. The Schiff base in the damaged nucleoside is attacked by an active-site lysine, resulting in the nucleoprotein intermediate.

Our data indicate that in a saturated pyrimidine residue, the Schiff base mechanism is favorable over the oxocarbenium ion pathway. Therefore, at least in the context of free nucleoside, the oxocarbenium ion may not be responsible for all deglycosylation processes. We wonder whether such a Schiff base intermediate may be utilized by DNA glycosylases in the BER pathway. BER enzymes can be divided into two categories: mono-functional BER enzymes which are DNA glycosylases that hydrolyze the *N*-glycosidic bond to yield an AP, and bi-functional BER enzymes which possess both glycosylase and AP lyase activities (Figure 8).[4] The oxocarbenium ion intermediate has long been suggested in mediating the deglycosylation process in mono-functional BER enzymes. Such a hypothesis was strongly supported by the kinetic isotope effect studies of the reaction catalyzed by uracil DNA glycosylase, which allowed the elucidation of the transition state configuration, suggesting that the reaction proceeds through a dissociative transition state, with complete dissociation of the uracil anion followed by

addition of water to the resulting oxocarbenium ion intermediate.[67]

In bi-functional enzymes, the ε-NH_2 of a lysine or the –NH of a proline is suggested to be added to the C1′ of the oxocarbenium ion intermediate, forming a Schiff base intermediate and removing the damaged nucleobase (Route A, Figure 8).[7,9] This Schiff base intermediate subsequently induces a β-elimination reaction, creating a nick at the 3′-side of the lesion. Some enzymes can even catalyze an additional δ-elimination, cleaving the 5′-end and generating a gap. In several bi-functional BER enzymes such as endonuclease III, multiple groups proposed that a Schiff base intermediate may be formed first at the *N*-glycosidic bond of the damaged base (Route B, Figure 8) before it reacts with an active site lysine.[9,37,38,68,69] Such a proposal however has not been accepted as the general mechanism because there is little experimental evidence demonstrating the existence of the Schiff base intermediate in DNA lesions other than Fapy•dG and Fapy•dA.[4] Our dHdU studies here indicate that at least in a saturated pyrimidine lesion like dHdU and dHT, the Schiff base intermediate is thermodynamically preferred over the oxocarbenium ion. Such an intermediate readily supports the lysine or proline mediated substitution reaction, generating the nucleoprotein Schiff base intermediate shown in Route B.

To establish this intriguing hypothesis, more DNA lesions need to be examined. As aforementioned, the purine N7 can be readily protonated, making it a good leaving group under the oxocarbenium ion pathway. It is known the 8-oxo-dG is repaired by bi-functional BER enzymes. If the above hypothesis is correct, 8-oxo-dG should support the Schiff base chemistry in the nucleoside context. Moreover, the involvement of the Schiff base intermediate in glycosylase catalysis may need to be checked by the transition state analysis using kinetic isotope effects similar to that conducted in uridine DNA deglycosylase.[67] To date, the transition state analyses were only performed in mono-functional BER enzymes.[4] Such an analysis should be conducted with bi-functional BER enzymes to obtain direct evidence on the nature of the reaction intermediate.

The dHdU isomerization results in two pairs of C1′ epimers, possessing a furanose and a pyranose respectively. Such a reaction is expected to occur in the oligonucleotide context as well. However, in an

oligonucleotide, the 5′-OH moieties are used to form the phosphodiester backbone. Therefore, in duplex genomic DNA, only α-furanose product **3**, the kinetically favorable product, may form; the ring expansion products **2** and **4** will not be generated. Although it is currently unknown whether the duplex DNA framework may slow down its formation, the fast formation rate (5.4×10^{-8} s^{-1}) at 37 °C and physiological pH observed here indicates that **3** may exist at a significant level in the genomic DNA of gamma irradiated cells where dHdU was found as a major DNA damage.[17] Consequently, considering that glycosylases are evolved by nature to repair the β-anomer of a modified nucleoside, any α-furanose product may not be able to fit in the enzyme binding pocket and thus cannot be repaired by BER enzymes. In such a case, the NER pathway may have to be involved as indicated by McKibbin et al..[10]

The nucleophilic addition by an active-site lysine to the C1′ of the nucleobase-harbored Schiff base intermediate leads to the formation of a nucleoprotein intermediate. Such a species was trapped by $NaBH_4$ treatment and characterized in a number of DNA glycosylases including endonuclease III, FPG, and Nei.[37,38,70,71] If dHdU and dHT are used as substrates for these enzymes, the Schiff base intermediate with the active site lysine residue may be formed (Route B, Figure 8). Formation of such species is feasible, as indicated by the production of the dHdU-cysteine adducts **6** and **7**. The formed lysine nucleoprotein complex however is not stable without the presence of the reductive trapping reagents as the Schiff base species can be readily hydrolyzed, re-generating the lysine residue. On the other hand, formation of **6** and **7** implies that the cysteine residue on a DNA binding protein may readily react with the Schiff base intermediate at a damaged nucleotide, resulting in a stable nucleoprotein complex. Both dHdU and dHT are known as major pyrimidine damages in γ-ray irradiated mammalian cells.[15,16] DNA-protein crosslinking reactions were observed during anoxic ionizing radiation of cells;[72] the molecular basis for these crosslinking reactions, however, remains unclear. The dHdU-thiol crosslinking studies reported here may provide some much needed mechanistic insight, and thus can be significant to the understanding of general radiation biology as well.

AUTHOR INFORMATION

Corresponding Author *Email: lilei@iupui.edu

Author Contributions ⊥These authors contributed equally.

Notes The authors declare no competing financial interest.

ACKNOWLEDGMENT The authors thank the National Institute of Health (R00ES017177 and R21AI097740), Foundation for Polish Science, and IUPUI startup funds for financial support. The NMR and MS facilities at IUPUI are supported by National Science Foundation MRI grants CHE-0619254 and DBI-0821661, respectively. The calculations were carried out in Wroclaw Center for Networking and Supercomputing, Grant No. 209.

Supporting Information Available: Characterizations of the dHT and dHdU adducts, ESI-MS analyses of the reaction intermediates. This information is available free of charge via the internet at http://pubs.acs.org.

REFERENCES

(1) Burrows, C. J.; Muller, J. G. *Chem. Rev.* **1998**, *98*, 1109.
(2) Greenberg, M. M. *Acc. Chem. Res.* **2011**, *45*, 588.
(3) Cadet, J.; Douki, T.; Gasparutto, D.; Ravanat, J.-L. *Mut. Res. Fund. Mol. Mech. Mut.* **2003**, *531*, 5.
(4) Berti, P. J.; McCann, J. A. B. *Chem. Rev.* **2006**, *106*, 506.
(5) Hegde, M. L.; Hazra, T. K.; Mitra, S. *Cell Res.* **2008**, *18*, 27.
(6) Norbury, C. J.; Hickson, I. D. *Ann. Rev. Pharmacol. Toxicol.* **2001**, *41*, 367.
(7) Zharkov, D. O.; Shoham, G.; Grollman, A. P. *DNA Repair* **2003**, *2*, 839.
(8) Stivers, J. T.; Jiang, Y. L. *Chem. Rev.* **2003**, *103*, 2729.
(9) McCullough, A. K.; Dodson, M. L.; Lloyd, R. S. *Ann. Rev. Biochem.***1999**, *68*, 255.
(10) McKibbin, P. L.; Fleming, A. M.; Towheed, M. A.; Van Houten, B.; Burrows, C. J.; David, S. S. *J. Am. Chem. Soc.* **2013**, *135*, 13851.
(11) Zoltewicz, J. A.; Clark, D. F.; Sharpless, T. W.; Grahe, G. *J. Am. Chem. Soc.* **1970**, *92*, 1741.
(12) Cadet, J.; Teoule, R. *J. Am. Chem. Soc.* **1974**, *96*, 6517.
(13) Shapiro, R.; Danzig, M. *Biochemistry* **1972**, *11*, 23.
(14) Lin, G.; Jian, Y.; Dria, K. J.; Long, E. C.; Li, L. *J. Am. Chem. Soc.* **2014**, *136*, 12938.
(15) Villanueva, J. M.; Pohl, J.; Doetsch, P. W.; Marzilli, L. G. *J. Am. Chem. Soc.* **1999**, *121*, 10652.
(16) Geacintov, N. E.; Broyde, S. *The chemical biology of DNA damage*; Wiley-VCH: Weinheim, 2010.
(17) Dizdaroglu, M.; Laval, J.; Boiteux, S. *Biochemistry* **1993**, *32*, 12105.
(18) Liu, J.; Doetsch, P. W. *Nucleic Acids Res.* **1998**, *26*, 1707.
(19) Liu, J.; Zhou, W.; Doetsch, P. W. *Mol. Cell Biol.* **1995**, *15*, 6729.
(20) *See supporting information*.
(21) Becke, A. D. *Phys. Rev. A* **1988**, *38*, 3098.

(22) Becke, A. D. *J. Chem. Phys.* **1993**, *98*, 5648.
(23) Lee, C. T.; Yang, W. T.; Parr, R. G. *Phys. Rev. B* **1988**, *37*, 785.
(24) Ditchfield, R.; Hehre, W. J.; Pople, J. A. *J. Chem. Phys.* **1971**, *54*, 724.
(25) Hehre, W. J.; Ditchfield, R.; Pople, J. A. *J. Chem. Phys.* **1972**, *56*, 2257.
(26) Frisch, M. J.; Trucks, G. W.; Schlegel, H. B.; Scuseria, G. E.; Robb, M. A.; Cheeseman, J. R.; Scalmani, G.; Barone, V.; Mennucci, B.; Petersson, G. A.; Nakatsuji, H.; Caricato, M.; Li, X.; Hratchian, H. P.; Izmaylov, A. F.; Bloino, J.; Zheng, G.; Sonnenberg, J. L.; Hada, M.; Ehara, M.; Toyota, K.; Fukuda, R.; Hasegawa, J.; Ishida, M.; Nakajima, T.; Honda, Y.; Kitao, O.; Nakai, H.; Vreven, T.; Montgomery Jr, J. A.; Peralta, J. E.; Ogliaro, F.; Bearpark, M. J.; Heyd, J.; Brothers, E. N.; Kudin, K. N.; Staroverov, V. N.; Kobayashi, R.; Normand, J.; Raghavachari, K.; Rendell, A. P.; Burant, J. C.; Iyengar, S. S.; Tomasi, J.; Cossi, M.; Rega, N.; Millam, N. J.; Klene, M.; Knox, J. E.; Cross, J. B.; Bakken, V.; Adamo, C.; Jaramillo, J.; Gomperts, R.; Stratmann, R. E.; Yazyev, O.; Austin, A. J.; Cammi, R.; Pomelli, C.; Ochterski, J. W.; Martin, R. L.; Morokuma, K.; Zakrzewski, V. G.; Voth, G. A.; Salvador, P.; Dannenberg, J. J.; Dapprich, S.; Daniels, A. D.; Farkas, Ö.; Foresman, J. B.; Ortiz, J. V.; Cioslowski, J.; Fox, D. J.; Gaussian, Inc., Gaussian 09, Revision D.01.: Wallingford, CT, USA, 2009.
(27) Miertuš, S.; Scrocco, E.; Tomasi, J. *Chem. Phys.* **1981**, *55*, 117.
(28) Miertuš, S.; Tomasi, J. *Chem. Phys.* **1982**, *65*, 239.
(29) Cossi, M.; Barone, V.; Cammi, R.; Tomasi, J. *Chem. Phys. Lett.* **1996**, *255*, 327.
(30) Wong, M. W.; Wiberg, K. B.; Frisch, M. *J. Chem. Phys.* **1991**, *95*, 8991.
(31) McQuarrie, D. A.; Simon, J. D. *Molecular thermodynamics*; University Science Books: Sausalito, Calif., 1999.
(32) Aumiller, J. C.; Whittle, J. A. *J. Org. Chem.***1976**, *41*, 2955.
(33) Casadei, M. A.; Galli, C.; Mandolini, L. *J. Am. Chem. Soc.* **1984**, *106*, 1051.
(34) Ma, B.; Schaefer, H. F.; Allinger, N. L. *J. Am. Chem. Soc.* **1998**, *120*, 3411.
(35) Juaristi, E.; Cuevas, G. *Tetrahedron* **1992**, *48*, 5019.
(36) Miller, N.; Cerutti, P. *Proc. Natl. Acad. Sci.* **1968**, *59*, 34.
(37) Zharkov, D. O.; Golan, G.; Gilboa, R.; Fernandes, A. S.; Gerchman, S. E.; Kycia, J. H.; Rieger, R. A.; Grollman, A. P.; Shoham, G. *EMBO J.* **2002**, *21*, 789.
(38) Gilboa, R.; Zharkov, D. O.; Golan, G.; Fernandes, A. S.; Gerchman, S. E.; Matz, E.; Kycia, J. H.; Grollman, A. P.; Shoham, G. *J. Biol. Chem.* **2002**, *277*, 19811.
(39) Gruber, T. D.; Westler, W. M.; Kiessling, L. L.; Forest, K. T. *Biochemistry* **2009**, *48*, 9171.
(40) Soltero-Higgin, M.; Carlson, E. E.; Gruber, T. D.; Kiessling, L. L. *Nat. Struct. Mol. Biol.* **2004**, *11*, 539.
(41) Miller, B. G.; Wolfenden, R. *Ann. Rev. Biochem.* **2002**, *71*, 847.
(42) Silverman, R. B.; [Rev. ed.] ed.; *The organic chemistry of enzyme-catalyzed reactions*; Academic Press: San Diego :, 2002.
(43) Kondo, Y.; Witkop, B. *J. Am. Chem. Soc.* **1968**, *90*, 764.
(44) Dinner, A. R.; Blackburn, G. M.; Karplus, M. *Nature* **2001**, *413*, 752.
(45) Jiang, Y. L.; Ichikawa, Y.; Song, F.; Stivers, J. T. *Biochemistry* **2003**, *42*, 1922.
(46) Frederico, L. A.; Kunkel, T. A.; Shaw, B. R. *Biochemistry* **1990**, *29*, 2532.
(47) Cannistraro, V. J.; Taylor, J.-S. *J. Mol. Biol.* **2009**, *392*, 1145.
(48) Lee, D.-H.; Pfeifer, G. P. *J. Biol. Chem.* **2003**, *278*, 10314.
(49) Lindahl, T. *Nature* **1993**, *362*, 709.
(50) Lindahl, T.; Nyberg, B. *Biochemistry* **1972**, *11*, 3610.
(51) Park, Y.; Li, Z.; Cloutier, P.; Sanche, L.; Wagner, J. R. *Radiat. Res.* **2011**, *175*, 240.
(52) Miljković, M. i.; Yeagley, D.; Deslongchamps, P.; Dory, Y. L. *J. Org. Chem.* **1997**, *62*, 7597.
(53) Larsen, C. H.; Ridgway, B. H.; Shaw, J. T.; Woerpel, K. A. *J. Am. Chem. Soc.* **1999**, *121*, 12208.
(54) Woods, R. J.; Andrews, C. W.; Bowen, J. P. *J. Am. Chem. Soc.* **1992**, *114*, 859.
(55) Gloster, T. M.; Vocadlo, D. J. *Nat. Chem. Biol.* **2012**, *8*, 683.

(56) Kelley, J. A.; Driscoll, J. S.; McCormack, J. J.; Roth, J. S.; Marquez, V. E. *J. Med. Chem.* **1986**, *29*, 2351.
(57) Everse, J.; Anderson, B.; You, K.-s. *The Pyridine nucleotide coenzymes*; Academic Press: New York, 1982.
(58) Klemm, A.; Steiner, T.; Flotgen, U.; Cumme, G. A.; Horn, A. *Methods Enzymol.* **1997**, *280*, 171.
(59) Montgomery, J. A.; Thomas, H. J. *J. Org. Chem.* **1971**, *36*, 1962.
(60) Ferris, J. P.; Singh, S.; Newton, T. A. *J. Org. Chem.* **1979**, *44*, 173.
(61) Haraguchi, K.; Delaney, M. O.; Wiederholt, C. J.; Sambandam, A.; Hantosi, Z.; Greenberg, M. M. *J. Am. Chem. Soc.* **2002**, *124*, 3263.
(62) Haraguchi, K.; Greenberg, M. M. *J. Am. Chem. Soc.* **2001**, *123*, 8636.
(63) Jiang, Y. L.; Wiederholt, C. J.; Patro, J. N.; Haraguchi, K.; Greenberg, M. M. *J. Org. Chem.* **2004**, *70*, 141.
(64) Burgdorf, L. T.; Carell, T. *Chem. Eur. J.* **2002**, *8*, 293.
(65) Raoul, S.; Bardet, M.; Cadet, J. *Chem. Res. Toxicol.* **1995**, *8*, 924.
(66) Chen, X. Y.; Berti, P. J.; Schramm, V. L. *J. Am. Chem. Soc.* **2000**, *122*, 1609.
(67) Werner, R. M.; Stivers, J. T. *Biochemistry* **2000**, *39*, 14054.
(68) Kow, Y. W.; Wallace, S. S. *Biochemistry* **1987**, *26*, 8200.
(69) Purmal, A. A.; Rabow, L. E.; Lampman, G. W.; Cunningham, R. P.; Kow, Y. W. *Mutat. Res.* **1996**, *364*, 193.
(70) Sun, B.; Latham, K. A.; Dodson, M. L.; Lloyd, R. S. *J. Biol. Chem.* **1995**, *270*, 19501.
(71) Fromme, J. C.; Verdine, G. L. *EMBO J.* **2003**, *22*, 3461.
(72) Barker, S.; Weinfeld, M.; Zheng, J.; Li, L.; Murray, D. *J. Biol. Chem.* **2005**, *280*, 33826.

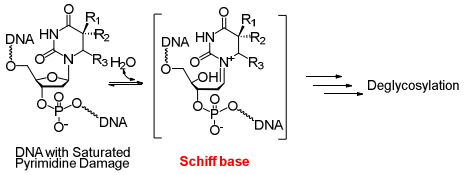
DNA
HN
O
N
R1
R2
R3
H2O
OH
DNA with Saturated Pyrimidine Damage
Schiff base
Deglycosylation